Neural Network Noise Prediction for a Complex Supersonic Rectangular Jet Nozzle

Seth W. Kelly*, Tyler M. Vartabedian†, Emma D. Gist‡, and Mark N. Glauser§
Syracuse University, Syracuse, NY, 13244, USA

A method for the prediction of far-field acoustics emanating from a complex supersonic rectangular nozzle using machine learning techniques is presented. Complexity and lengthy times associated with traditional experimental and numerical procedures motivate the use of a rapid noise prediction system based on modern machine learning computational methods. An artificial neural network (ANN) is employed to predict the far-field overall sound pressure levels (OASPL) for a Multi Aperture Rectangular Single Expansion Ramp Nozzle (MARS). A combination of experimental techniques and machine learning algorithms are utilized. The results yield a simple, accurate, and computationally frugal method for the prediction of far-field acoustic magnitudes and directions. Realistic operating conditions and geometric properties serve as inputs to this model which calculates OASPL at multiple far-field locations. This provides a basis for further exploration of geometric modifications and passive control schemes while continuing to explore the effects of a newly installed splitter plate trailing edge (SPTE) geometry. Preliminary Large Eddy Simulation (LES) data performed by The Ohio State University have shown that the introduction of a spanwise wavenumber to the SPTE results in a reduction of the 34 kHz tone associated with the shedding frequency of the splitter plate. With this dominating tone greatly reduced, a more in depth study into the acoustic effects of different aft deck lengths can be performed and ultimately optimized for a desired acoustic output.

I. Nomenclature

LES	=	Large Eddy Simulation
$SPTE$	=	Splitter Plate Trailing Edge
PIV	=	Particle Image Velocimetry
NPR	=	Nozzle Pressure Ratio
NTR	=	Nozzle Temperature Ratio
$SERN$	=	Single Expansion Ramp Nozzle
$MARS$	=	Multi-Aperture Rectangular SERN
$SBLI$	=	Shockwave Boundary Layer Interactions
D_h	=	Hydraulic Diameter
β	=	Spanwise Wavenumber
ANN	=	Artificial Neural Network
DNN	=	Deep Neural Network
NN	=	Neural Network
$OASPL$	=	Overall Sound Pressure Level
dB	=	Decibels
L_d	=	Aft Deck Length
$RMSE$	=	Root Mean Square Error
$MAPE$	=	Mean Absolute Percentage Error

*Department of Mechanical and Aerospace Engineering, Syracuse University, AIAA Student Member
†Department of Mechanical and Aerospace Engineering, Syracuse University, AIAA Student Member
‡Department of Mechanical and Aerospace Engineering, Syracuse University, AIAA Student Member
§Professor, Department of Mechanical and Aerospace Engineering, AIAA Fellow

II. Introduction

The aerospace industry continues to develop more advanced engines to improve aircraft capabilities and performance [1]. The goal of flying faster and further has been enabled by the incorporation of complex nozzles. Design alterations to these complex nozzles have utilized multiple high-velocity streams ejected through a non-axisymmetric exit. An example of a modern design featuring a Single Expansion Ramp Nozzle (SERN) in a variable cycle engine was discussed by Simmons [1] (see Figure 1). This features a rectangular SERN with an additional bypass stream.

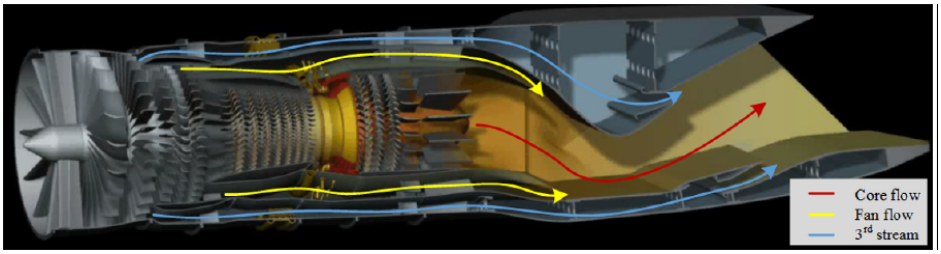

Fig. 1 Variable Cycle Engine by Simmons [1].

This configuration has been shown to allow for decreased pressure drag compared to axisymmetric nozzles [2], incorporated thrust vectoring [3], and improved off-design performance [1]. The system includes a secondary bypass stream, referred to as the 3rd stream in this study. This cold, low pressure stream protects the aft-deck from the hot core (combination of the fan and first bypass streams) stream while reducing noise and the resulting drag [4]. The fundamental flow physics of this model have been explored utilizing a Multi-Aperture Rectangular SERN (MARS) at Syracuse University (see Figure 2) .

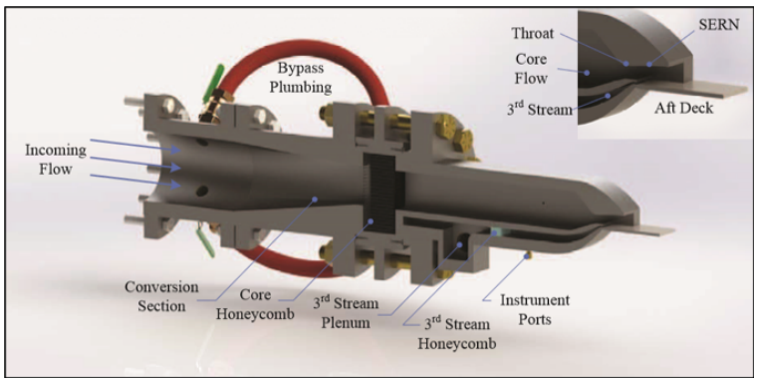

Fig. 2 Cross-Section Rendering of MARS Jet [5]

The MARS separates the two canonical flows via a splitter plate with nominal conditions of Nozzle Pressure Ratio (NPR) of 4.25 for the core flow and 1.89 for the 3rd stream (Mach 1.6 and 1.0, respectively). This supersonic operating condition results in a complex, turbulent environment dominated by an acoustic emission centered around 60° from the jet axis. Multiple studies,[5], [6], [7], [8], [9] have showed this instability compromises the beneficial effects of the complex system. This has been attributed to the mixing of the two flows downstream of the splitter plate trailing edge (SPTE). Generating a complex vortex shedding instability that deflects down into the aft-deck plate boundary layer and propagates downstream. The varied-density streams, along with the supersonic nature of the nominal operating conditions, create a series of reflected shock trains and expansion waves. These complex characteristics reflect off the MARS, the aft-deck plate, and the resulting shear layers at the exit of the nozzle. Figure 3 shows the aerodynamic features as described. This complex shock structure generates an assortment of noise that propagates downstream into the far-field. Turbulent mixing noise is generated by the interaction of vortical structures produced by mean shear in the jet, and jet screech is produced when the upstream propagating part of the acoustic field creates a feedback loop with fluctuations originating at the nozzle lip [7].

Major flow characteristics have been simulated using Large Eddy Simulations (LES) by Stack *et al* [8] and experimentally verified by Berry *et al* [5], and Magstadt [7]. Gist *et al* [10] expanded upon these prior results while

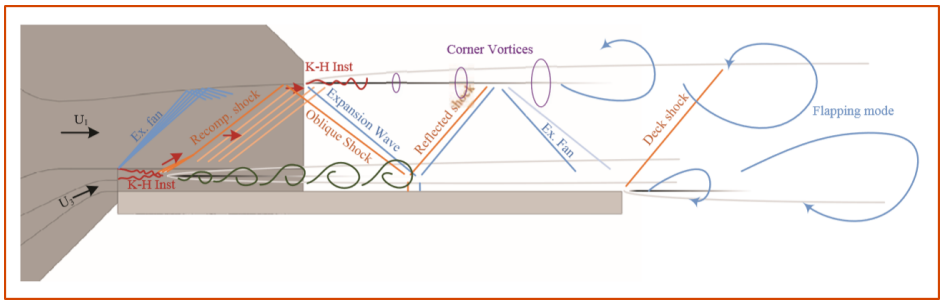

Fig. 3 MARS Flow Structure [6].

continuing to explore the aft-splitter plate region and resulting instabilities. Specifically, the splitter plate shedding instability was explored in depth by Stack & Gaitonde [9]. Simulations have been shown that altering this splitter plate thickness reduces the energies associated with the resulting shear instabilities [11]. The varied shear conditions were also found to impact the directionality of the far-field noise in the sideline plane [12]. Although the OASPL is dominated by a characteristic 34 kHz (for the nominal case) instability and has been heavily studied, other noise-inducing instabilities have yet to be targeted for optimization. Low-frequency components (<10,000 Hz) outside of the jet and in the far field are tied to the dynamics associated with the bulk flow [12]. These complex, reflected interactions can be impacted by the surrounding geometries of the splitter plate and the aft-deck plate. However, they are difficult to analyze due to the larger presence of the SPTE instability.

Gist *et al* [13] recently proposed a new splitter plate geometry that introduces a sinusoidal pattern to the SPTE. The induced wavenumber $\beta = 0.8$ was determined by the High-Fidelity Computational Multi-Physics Laboratory at The Ohio State University to effectively reduce the energy associated with the splitter plate shearing instability [13] and the resulting noise. This new SPTE is shown in Figure 4. The spike shown in Figure 5 has been effectively eliminated when employing this wave induced SPTE [13]. Ruscher *et al* [14] found that reducing the thickness of the SPTE had a similar effect, but the wavy SPTE simulations promise more ideal results. The thickness remains the same in the new splitter plate to focus on only the effects from the induced waveform. The sinusoidal SPTE geometry leads the two streams to mix faster, following the formation of streamwise vortex structures and their subsequent interference with spanwise vortices in the shear layer.

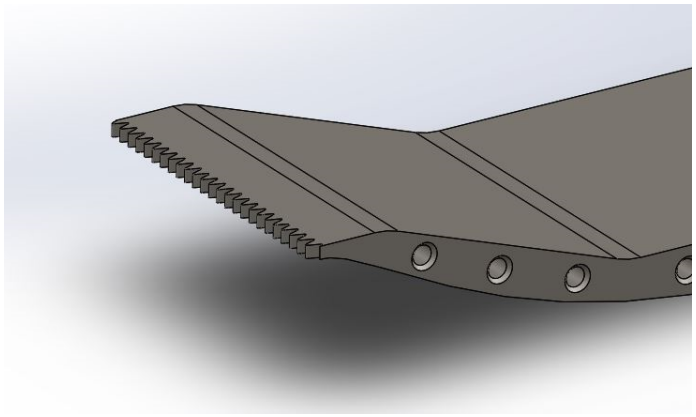

Fig. 4 CAD file for the new SPTE geometry for $\beta = 0.8$. [13]

Tenney *et al* [12, 15] applied data fusion and modern computational techniques to develop a rapid far-field overall sound pressure level (OASPL) prediction algorithm for the nominal MARS geometric configuration. The resulting neural network supplements the inability to collect time-resolved full-field velocity measurements. This is due to the short timescales associated with the flow from the MARS nozzle in its current configuration. This was the first application of machine learning to this system and serves as a basis for this study. Tenney showed that machine learning methods can predict acoustics at the same accuracy when compared to linear stochastic estimation. Typically, Ffowcs Williams-Hawkings (FWH) surfaces are used in conjunction with CFD models to estimate far-field noise [12]. This

ensures that a NN is a viable option for exploring and relating characteristics of supersonic flows. Tenney's [12] artificial neural network (ANN) is expanded upon in this study to provide a rapid OASPL prediction technique for the newly installed splitter plate. The original ANN predicts OASPL magnitudes to within ±4 dB and correct directionality utilizing simple operating parameters and geometric properties for inputs [12].

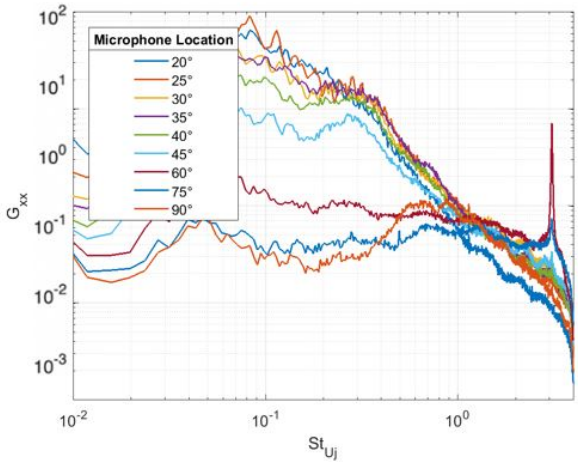

Fig. 5 Acoustic Spectra for Nominal Conditions and Nominal Aft-Deck Plate.

The purpose of this study is to further the development of this existing neural network for implementation with the newly designed SPTE geometry in Figure 4. This can be done by retraining a modified version of the NN following the installation of the new splitter plate. The results will yield a fast and simple prediction method for overall sound pressure magnitudes and directionalities. Following this, geometric modifications to the MARS will be explored. Specifically, the aft-deck plate geometry will be optimized for different operating conditions using predictions from the NN. In the absence of the dominating SPTE instability, more focus can be applied to the lower-frequency tones directly impacted by the aft-deck lengths.

III. Experimental Methods

Modern computational machine learning methods are applied and used in conjunction with experimental techniques. Fusing the strengths of both allows for validation of results and further training of the NN. Experimental measurements are recorded to provide training data for the NN and verify its accuracy. These methods encompass a variety of basic flow inputs with differing aft-deck plate lengths. The OASPL data is recorded, processed and acts as targets for the NN.

All experiments are performed in the Skytop Turbulence Laboratories anechoic chamber located at Syracuse University's south campus. This 206 m^3 acoustically treated chamber features near-field dynamic pressure transducers, a particle image velocimetry (PIV) setup, and a far-field acoustic array. The facility is fitted with 10 far-field microphones to capture acoustics at a rate of 100 kHz per channel. The facility is shown in Figures 6 and 7.

This experimental facility allows for an easily modifiable test environment. Basic flow characteristics can be changed along with varied aft-deck plate geometries efficiently. Flow characteristics altered include the primary stream nozzle ratio (NPR_1), third stream nozzle pressure ratio (NPR_3), and the nozzle temperature ratios (NTR). Previous efforts focused on capturing the flow for a wide range of operating conditions [12]. This campaign narrowed the focus to a wider range of deck plate lengths and a constant ratio between the NPRs. Furthermore the total number of test runs conducted with the new SPTE was increased from 300 to 503 and the number of different deck plates tested increased from 3 to 42. With the deck lengths (L_d) non-dimensionalized by the nozzle hydraulic diameter D_h = 44.5 mm, and decks varying in length by steps of 0.1 L_d/D_h. Some example aft-deck plate geometries are shown in Figure 8.

To train the neural network, 503 test runs are performed with 10 second sampling increments. The sampled acoustic data is post processed to calculate the OASPL. The noise model domain for the collected training and validation data from the previous and current studies can be seen in Figure 9a and 9b respectively. The markers are scaled by the length of the aft-deck plate, with the smallest corresponding to the no deck case. They are also colored to represent the NTR of the core stream. The shift from the data set over a wide range of operating conditions towards the larger data set with

Fig. 6 Anechoich Chamber at Skytop Turbulence Laboratories, Syracuse NY.

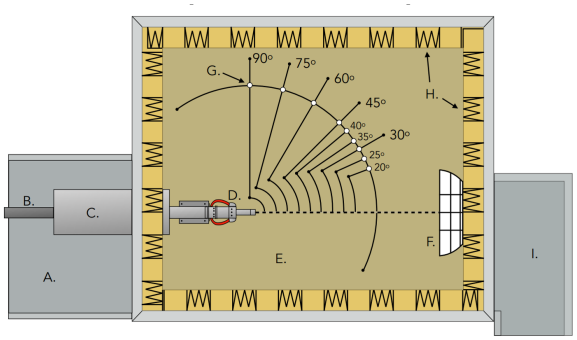

Fig. 7 Anechoic Chamber Layout: ***A. Plenum Chamber, B. Jet Feed Pipe (to compressed air tanks), C. Bypass Air Flow Straightener, D. Jet Rig, E. Anechoic Chamber, F. Plume Catcher, G. Far- Field Condenser Microphones, H. Acoustic Fiberglass Wedges, I. Exhaust Path*** **[6].**

Fig. 8 Example aft-decks (left) and mounted aft-deck (right)

less variation between the operating conditions and more deck plates allowed for an increased focus into the effects that the aft deck length has on the acoustic output of the system.

The far-field acoustic microphone array is used to capture the acoustics in the same plane as the SERN. The 10 microphones are G.R.A.S. 46BE free-field condenser microphones and feature a dynamic range of 160 dB with a noise floor of 30 dB. The microphones are setup in 15°increments from 90°to 20°from the jet axis in a semi-circular arc 86.6 D_h from the nozzle exit plane.

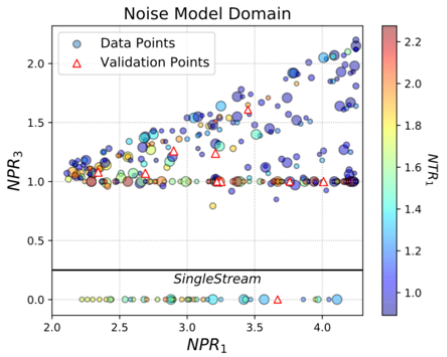

(a) Noise Model Domain previous SP [12]

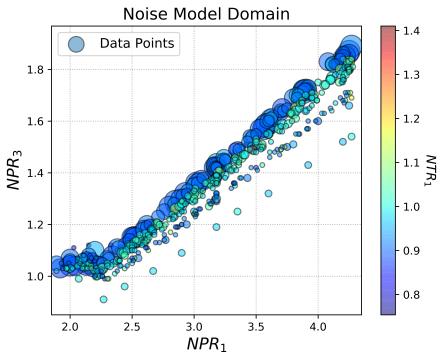

(b) Current Noise Model Domain

IV. Machine Learning Computational Methods

A neural network is employed for this project. The NN utilized Python with Pytorch. These were chosen due to their ease of use and proven abilities.

A simulation approach is utilized with the neural network. As explained prior, this NN outputs OASPL magnitudes and directionalities, while inputting basic flow and geometric parameters. Neural networks consist of artificial neurons connected to each other with assigned weights and biases. Deep neural networks (DNN) expand upon an ANN by adding additional hidden layers. At each layer, a summation of the linear combinations of input variables is given by:

$$s = XW + b \tag{1}$$

With a nonlinear activation function example given as:

$$f(s) = \frac{1}{1 + e^{-s}} \tag{2}$$

For this neural network, Rectified Linear Units, or ReLU activation function is utilized. This was done to avoid the possible vanishing gradient problem with sigmoid activations [12]. To train the network, a backpropagation algorithm is used. The initial weights and biases between each node are randomly generated. These values are tweaked by training the algorithm, where the experimentally determined output is compared to the initially generated output. This comparison calculates the error as root mean squared error (RMSE). The network cycles through epochs until the error reaches a global minimum. The backpropagation is updated using the following equation:

$$w_{kj}^{i+1} = w_{kj}^{i} - \alpha \frac{\delta C}{\delta w_{kj}} \tag{3}$$

Where w_{kj} is an element of the weight matrix, C is the cost function, and α is the learning rate. The weights for this neural network are updated using gradient descent. The inputs to the model are restricted to simple, non-dimensional geometric and flow conditions. This allows for analysis of possible contributors to noise parameters common to the nozzle design process. The feature space is shown in Table 1.

Input Feature
NPR_1
NPR_3
L_d/D_h
$T_1/273K$
NTR_1
NTR_3

Table 1 Features of Predictive Neural Network

OASPL is calculated by integrating the frequency dependent sound pressure level (SPL), with the frequency non-dimensionalized by the hydraulic diameter D_h and and the jet exit velocity U_j.

$$OASPL = \int SPL(f)df \tag{4}$$

Where the frequency dependent sound pressure level is given by:

$$SPL(f) = 20\log_{10}\frac{P_{\text{rms}}(f)}{P_{\text{ref}}}dB \tag{5}$$

And P_{ref} was 20 μPa. The current neural network settings are summarized in Table 2:

Hidden Layers	2
Nodes	500
Train/Test Split	80/20
Training Epochs	5000
Hidden Activations	ReLU
Kernel Initializer	Random Normal
Objective	Mean Squared Error
Optimizer	Adam
Learning Rate	0.001

Table 2 Neural Network Settings

V. Results

A. Verifying NN Accuracy

The neural network is shown to correctly predict OASPL to within 1.6 dB at its worst with most results falling within ±0.6 dB. This showed an improvement from the previous model that predicted OASPL to within 4 dB at its worst with most results falling within ±1 dB [12]. The NN also correctly predicts the direction of peak noise as well as trends in directionality.The peak noise emission directs consistently to 25° from the jet axis as expected. Figure 10 shows the predicted results versus experimentally determined results for two random test cases. This clearly shows the accuracy of both predicted magnitudes and directionality of the NN.

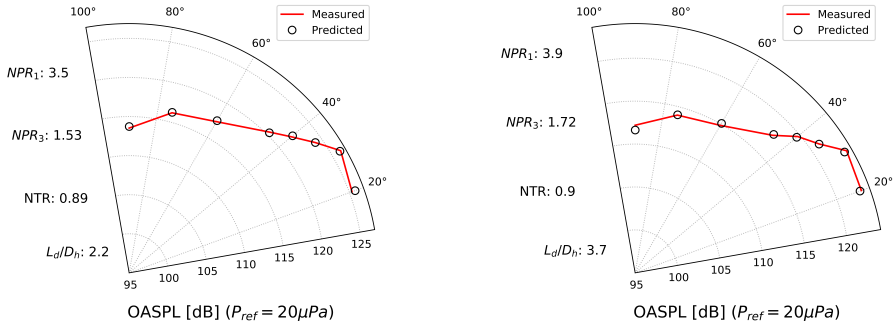

Fig. 10 OASPL Predictive Results

To further increase the confidence in the Neural Networks predictive capabilities, K-fold cross validation is performed with k = 10. The testing/training data is split into k equal parts. On these parts or "folds" training/testing is performed in k iterations such that within each iteration one fold is used for testing while the other 9 are trained on. This process

seeks to eliminate bias within the overall regression model and ensure its ability to correctly predict future data in addition to providing an adequate fit of the testing data [16]. The average testing and training RMSE from the k-fold cross validation as well as the overall MAPE for the regression model can be seen in Table 3

K-fold Training $RMSE$	0.674 dB
K-fold Testing $RMSE$	0.712 dB
Overall $MAPE$	0.43 %

Table 3 NN Error Metrics

B. Predicting New Deck Plates

As an additional method to verify the accuracy of the NN model and to test its ability to act as a complete model of how the farfield acoustics are affected with a changing deck length, three additional deck plates were manufactured. The decks, measuring L_d/D_h = 0.76, 1.86, and 2.64 respectively had lengths that lied in between those that the model was originally trained/tested on. Tests are conducted on these deck plates with common operating conditions and the farfield OASPLs recorded. Furthermore these new deck lengths were fed into the NN model with those same nozzle parameters. Figure 12 shows the measured and predicted OASPL values for these deck plates that the NN has never seen before. The NN was able to correctly capture the trend of the data with a marginally lower accuracy , MAPE for these trials was 0.55%. The microphone that showed the highest error was located at 60°from the jet plume. Past research has shown this microphone to be the most susceptible to picking up the tones related to the shedding frequency of the splitter plate as the jet nears the nominal operating conditions [12]. The inaccuracy of the model with this microphone in particular could relate back to the modifications made to the SPTE.

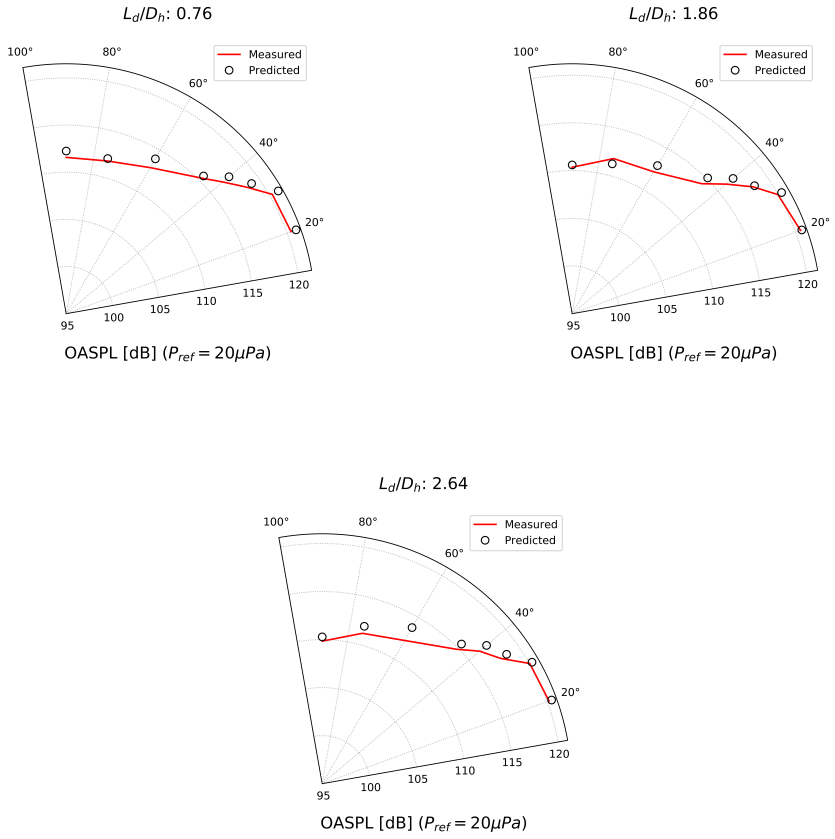

Fig. 12 OASPL Predictive Results for new deck lengths

C. Exploring Different Aft Deck Lengths

With the NN proven to be accurate within 99.6 % when predicted OASPL for the far-field acoustics a study into the effects of the aft deck length is conducted. Figure 13 shows the predicted average OASPL for all 42 deck plates tested over a range of operating conditions. As expected increasing the NPR_1 leads to an increase in OASPL for all deck plates. The relationship between the deck length and the average OASPL is not simply linear. Across all of the different operating conditions tested the variation of average OASPL with respect to deck length was relatively minor. However, there is indication of a slight periodic relationship between these variables. At lower speeds the quietest deck plate length is the longest. As the NPR_1 approaches 4.25, coinciding with a Mach 1.6 core flow, the minimum noise deck lengths shifts towards a L_d/D_h of 1.8.

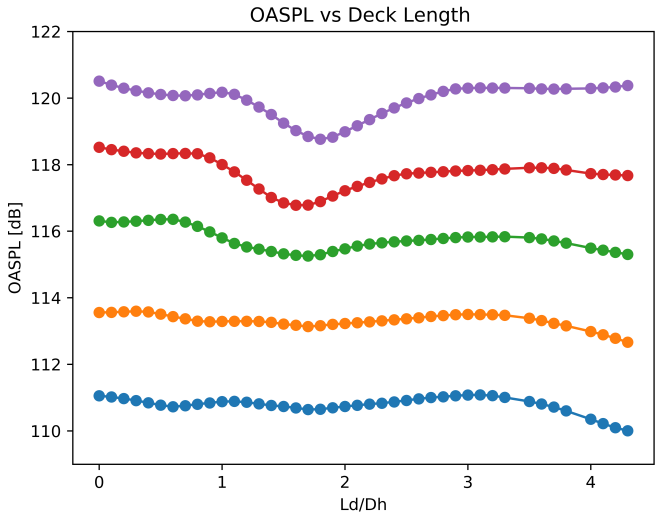

NPR1	1st Stream Mach #
4.25	1.6
3.67	1.5
3.18	1.4
2.77	1.3
2.43	1.2

Fig. 13 Variation between OASPL for all decks over different operating conditions

VI. Conclusions and Future Work

To understand the effects of the newly implemented wave number to the splitter plate trailing edge within a Multi Aperture Single Expansion Ramp Nozzle and create a model that can predict far-field OASPL for a variety of operating conditions and aft deck lengths an Artificial Neural Network (ANN) was used. This ANN consisted of 4 layers: input, output and 2 hidden layers. A large data set consisting of 503 test runs and 42 different aft deck lengths was supplied to Neural Network (NN). The NN was shown to accurately predict the OASPL for a variety of deck lengths and operating conditions. The NN model was also shown to effectively predict OASPL for deck lengths that it has never seen before. With the accuracy of the model verified the relationship between the deck length and OASPL over different operating conditions was investigated. It was shown that the relationship between these two values is not linear, and exhibits a slight periodic pattern. Furthermore the minimum noise configuration across nozzle operating conditions is not a constant.

Additional test runs are to be performed to expand the data set utilized in the NN training . Specifically test runs at higher temperature ratios, runs with a varied relationship between the first and third stream NPR's, as well as more runs near the nominal operating conditions. More runs at these conditions will allow for additional comparisons of the OASPL findings with existing PIV databases that require higher temperatures than the runs conducted in this study. PIV will allows a look into the flow physics and shock structure of the nozzle perhaps providing insight into the periodic nature of the deck length and OASPL. Furthermore a fusion of previous data with the nominal SPTE with current data of the SPTE with a wavenumber into a single Deep Neural Network could provide insight into the differences between the configurations with respect to the OASPL.

Acknowledgments

This study was provided funding via research grants by the Air Force Office of Scientific Research (AFOSR) grant number FA9550-19-1-0081. A special thanks to the entire Skytop Turbulence Laboratories group for their help and input to this project. A big thanks to Dr. Andrew S. Tenney for the development of the original predictive neural network that served as a basis for this project, and for introducing machine learning to Skytop Labs.

References

[1] Simmons, R. J., "Design and control of a variable geometry turbofan with and independently modulated third stream," Ph.D. thesis, The Ohio State University, 2009.

[2] CAPONE, F., "The nonaxisymmetric nozzle-It is for real< 149> fighter aircraft performance viewpoint," *Aircraft Systems and Technology Meeting*, 1979, p. 1810.

[3] Deere, K., and Asbury, S., "An experimental and computational investigation of a translating throat single expansion-ramp nozzle," *32nd Joint Propulsion Conference and Exhibit*, 1996, p. 2540.

[4] Bruening, G. B., and Chang, W. S., "Cooled cooling air systems for turbine thermal management," *ASME 1999 International Gas Turbine and Aeroengine Congress and Exhibition*, American Society of Mechanical Engineers Digital Collection, 1999.

[5] Berry, M. G., Stack, C. M., Magstadt, A. S., Ali, M. Y., Gaitonde, D. V., and Glauser, M. N., "Low-dimensional and data fusion techniques applied to a supersonic multistream single expansion ramp nozzle," *Phys. Rev. Fluids*, Vol. 2, 2017, p. 100504. https://doi.org/10.1103/PhysRevFluids.2.100504, URL https://link.aps.org/doi/10.1103/PhysRevFluids.2.100504.

[6] Berry, M. G., "Investigating the Interaction of a Supersonic Single Expansion Ramp Nozzle and Sonic Wall Jet," Ph.D. thesis, Syracuse University, 2016.

[7] Magstadt, A. S., "Investigating the Structures of Turbulence in a Multi-Stream, Rectangular, Supersonic Jet," Ph.D. thesis, Syracuse University, 2017.

[8] Stack, C. M., Gaitonde, D. V., Agostini, L., Berry, M. G., Magstadt, A. S., and Glauser, M. N., "Numerical investigation of a supersonic multistream jet with an aft-deck," *54th AIAA Aerospace Sciences Meeting, 2016*, American Institute of Aeronautics and Astronautics Inc, AIAA, 2016.

[9] Stack, C. M., and Gaitonde, D. V., "Shear Layer Dynamics in a Supersonic Rectangular Multistream Nozzle with an Aft-Deck," *AIAA Journal*, Vol. 56, No. 11, 2018, pp. 4348–4360.

[10] Gist, E. D., and Glauser, M. N., *On the Control of a Rectaungular Supersonic Multistream Flow Using Spanwise Geometric Modifications*, American Institute of Aeronautics and Astronautics Inc, AIAA, 2020.

[11] Ruscher, C. J., Magstadt, A. S., Berry, M. G., Glauser, M. N., Shea, P. R., Viswanath, K., Corrigan, A., Gogineni, S., Kiel, B. V., and Giese, A. J., "Investigation of a Supersonic Jet from a Three-Stream Engine Nozzle," *AIAA Journal*, Vol. 56, No. 4, 2018, pp. 1554–1568.

[12] Tenney, A. S., "Modern Methods in Machine Learning as Applied to the Study of a Complex Supersonic Jet Flow," Ph.D. thesis, Syracuse University, 2019.

[13] Gist, E., Doshi, P., Kelly, S., Glauser, M., and Gaitonde, D., "Exploratory Passive Control Study of a Supersonic Multi-Stream Nozzle Flow," *2020 AIAA AVIATION Meeting*, 2020.

[14] Ruscher, C. J., Gogineni, S., and Ferrill, T., "Splitter Plate Edge Effects in a Supersonic Multi-stream Nozzle," *2018 Joint Propulsion Conference*, 2018, p. 4745.

[15] Tenney, A., Glauser, M., Ruscher, C., and Berger, Z., "Application of Artificial Neural Networks to Stochastic Estimation and Jet Noise Modeling," *AIAA Journal*, Vol. 58, 2020, pp. 1–12. https://doi.org/10.2514/1.J058638.

[16] Yadav, S., and Shukla, S., "Analysis of k-Fold Cross-Validation over Hold-Out Validation on Colossal Datasets for Quality Classification," *2016 IEEE 6th International Conference on Advanced Computing (IACC)*, 2016, pp. 78–83. https://doi.org/10.1109/IACC.2016.25.